Article

STM Studies of Fusion of Cholesterol Suspensions and Mixed 1,2-Dimyristoyl-*sn*-glycero-3-phosphocholine (DMPC)/Cholesterol Vesicles onto a Au(111) Electrode Surface

Slawomir Sek, Shimin Xu, Maohui Chen, Grzegorz Szymanski, and Jacek Lipkowski

J. Am. Chem. Soc., **2008**, 130 (17), 5736-5743 • DOI: 10.1021/ja711020q • Publication Date (Web): 05 April 2008

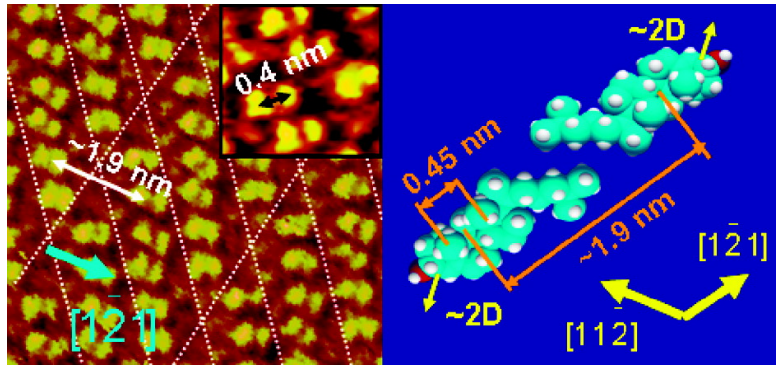

More About This Article

Additional resources and features associated with this article are available within the HTML version:

- Supporting Information
- Links to the 1 articles that cite this article, as of the time of this article download
- Access to high resolution figures
- Links to articles and content related to this article
- Copyright permission to reproduce figures and/or text from this article

View the Full Text HTML

J|A|C|S
ARTICLES

Published on Web 04/05/2008

STM Studies of Fusion of Cholesterol Suspensions and Mixed 1,2-Dimyristoyl-*sn*-glycero-3-phosphocholine (DMPC)/ Cholesterol Vesicles onto a Au(111) Electrode Surface

Slawomir Sek, Shimin Xu, Maohui Chen, Grzegorz Szymanski, and Jacek Lipkowski*

Department of Chemistry, University of Guelph, Guelph, Ontario, N1G 2W1, Canada

Received December 11, 2007; E-mail: jlipkows@uoguelph.ca

Abstract: Electrochemical scanning tunneling microscopy (EC-STM) has been applied to study the structure of the film formed by fusion of cholesterol suspensions and mixed dimyristoylphosphatidylcholine (DMPC)/ cholesterol vesicles on a Au(111) electrode surface. It has been demonstrated that cholesterol molecules assemble at the gold support into several structures templated by the crystallography of the metal surface and involving flat or edge-on adsorbed molecules. Studies of the film formed by fusion of mixed DMPC/ cholesterol vesicles revealed that ordered domains of either pure DMPC or pure cholesterol were formed. These results indicate that, at the metal surface, the molecules released by the rupture of a vesicle initially self-assemble into a well-ordered monolayer. The self-assembly is controlled by the hydrocarbon skeleton−metal surface interaction. In the case of mixed DMPC/cholesterol vesicles, the molecule−metal interactions induce segregation of the two components into single component domains. However, the molecule−metal interaction induced monolayer is a transient phenomenon. When more molecules accumulate at the surface, the molecule−molecule interactions dominate the assembly, and the monolayer is transformed into a bilayer.

Introduction

Solid supported phospholipid bilayers (SPBs) create artificial biofunctional surfaces[1–5] mimicking biological membranes. The SPBs can be formed by a spontaneous fusion of phospholipid vesicles onto a solid substrate.[6] Because of its simplicity, this is a very popular method of SPB formation. The mechanism of spreading vesicles at glass, quartz, mica, and mercury has been investigated intensively.[7–20] These studies determined that at hydrophilic surfaces the mechanism of vesicle spreading involves several consecutive steps such as vesicle adsorption, rupture, fusion, and movements of fragments of the bilayer at the solid surface by sliding or rolling by a tank-tread like motion.[3,8,19] It has also been established that the kinetics of vesicle fusion is controlled by mass transport, temperature, size, and composition of vesicles, nature of the solid surface, and the presence of ions in solution. For a recent review see Richter et al.[19]

The SPBs can also be formed by vesicle fusion on hydrophobic surfaces of metals such as gold.[22–26] As a result, they can be utilized for the development of biosensors.[27] In contrast to hydrophilic surfaces, the mechanism of vesicles spreading at gold[28] or mercury[14,15] is much less understood as illustrated by a recent discussion.[16] The knowledge concerning interactions

(1) Bayerl, M. M.; Bloom, T. *Biophys. J.* **1990**, *58*, 357.
(2) Schmidt, A.; Spinke, J.; Bayerl, T; Sackmann, E.; Knoll, W *Biophys. J.* **1992**, *63*, 1385.
(3) Sackmann, E. *Science* **1996**, *271*, 43.
(4) Williams, L. M.; Evans, S. D.; Flynn, T. M.; Marsh, A.; Knowles, F. R.; Bushby, J.; Boden, N. *Langmuir* **1997**, *13*, 751.
(5) Fisher, M. I.; Tjarnhage, T. *Biosens. Bioelectron.* **2000**, *15*, 463.
(6) Watts, T. H.; Brian, A. A.; Kappler, J. W.; Marrack, P.; McConell, H. M. *Proc. Natl. Acad. Sci. U.S.A.* **1984**, *81*, 7564.
(7) Lipowsky, R.; Seifert, U. *Mol. Cryst. Liq. Cryst.* **1991**, *202*, 17.
(8) Raedler, J.; Strey, H.; Sackmann, E. *Langmuir* **1995**, *11*, 4539.
(9) Seifert, U. *Adv. Phys.* **1997**, *46*, 13.
(10) Keller, C. A.; Kasemo, B. *Biophys. J.* **1998**, *75*, 1397.
(11) Reviakine, I.; Brisson, A. *Langmuir* **2000**, *16*, 1806.
(12) Zhdanov, V. P.; Kasemo, B. *Langmuir* **2001**, *17*, 3518.
(13) Seantier, B.; Breffa, C.; Felix, O.; Decher, G. *J. Phys. Chem. B* **2005**, *109*, 21755.
(14) Hellberg, D.; Scholz, F.; Schubert, F.; Lovric, M.; Omanovic, D.; Hernandez, V. A.; Thede, R. *J. Phys. Chem. B* **2005**, *109*, 14715.
(15) Hernandez, V. A.; Scholz, F. *Langmuir* **2006**, *22*, 10723.
(16) Zutic, V.; Svetlicic, V.; Zimmermann, A. H.; Ivosevic DeNardis, N.; Frkanec, R. *Langmuir* **2007**, *23*, 8647.
(17) Jass, J.; Tjarnhage, T.; Puu, G. *Biophys. J.* **2000**, *79*, 3153.
(18) Oncins, G.; Picas, L.; Hernandez-Borrell, J.; Garcia-Manyes, S.; Sanz, F. *Biophys. J.* **2007**, *93*, 2713.
(19) Richter, R. P.; Berat, R.; Brisson, A. R. *Langmuir* **2006**, *22*, 3497.
(20) (a) Majewski, J.; Wong, J. Y.; Park, C. K.; Seitz, M.; Israelachvili, J. N.; Smith, G. S. *Biophys. J.* **1998**, *75*, 2363. (b) Wong, J. Y.; Majewski, J.; Park, C. K.; Seitz, M.; Israelachvili, J. N.; Smith, G. S. *Biophys. J.* **1999**, *77*, 1445.
(21) (a) Leonenko, Z. V.; Carnini, A.; Cramb, D. T. *Biochim. Biophys. Acta* **2000**, *1509*, 131. (b) Leonenko, Z. V.; Finot, E.; Ma, H.; Dahms, T. E. S.; Cramb, D. T. *Biophys. J.* **2004**, *86*, 3783. (c) Leonenko, Z. V.; Merkle, D.; Shamrakov, L. G.; Lees-Miller, S. P.; Cramb, D. T. *Biosensors and Bioelectronics* **2004**, *20*, 918. (d) Shamrakov, L. G.; Cramb, D. T. *Canadian J. Chem.* **2005**, *83*, 1190.
(22) Burgess, I.; Szymanski, G.; Li, M.; Horswell, S.; Lipkowski, J.; Majewski, J.; Satija, S. *Biophys. J.* **2004**, *86*, 1763.
(23) Burgess, I.; Szymanski, G.; Li, M.; Horswell, S.; Lipkowski, J.; Majewski, J.; Satija, S. *Colloids Surf., B* **2005**, *40*, 117.
(24) Bin, X.; Horswell, S. L.; Lipkowski, J. *Biophys. J.* **2005**, *89*, 592.
(25) Zawisza, I.; Lachenwitzer, A.; Zamlynny, V.; Horswell, S. L.; Goddard, J. D.; Lipkowski, J. *Biophys. J.* **2003**, *85*, 4055.
(26) Horswell, S. L.; Zamlynny, V.; Li, H.-Q.; Merril, A. R.; Lipkowski, J. *Faraday Discuss.* **2002**, *121*, 405.
(27) Koper, I. *Mol. Biosyst.* **2007**, *3*, 651.

10.1021/ja711020q CCC: $40.75

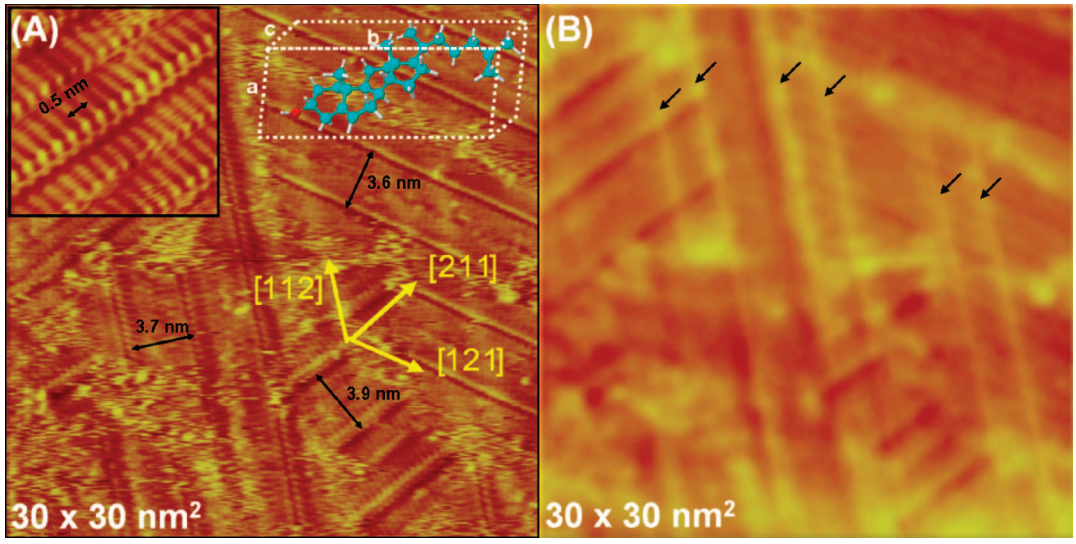

Figure 1. (a) Image of an Au(111) electrode surface acquired after injection of a cholesterol suspension to the STM cell. The crystallographic directions were determined from the orientation of the reconstruction lines on the underlying Au(111) surface. Insets show the high-resolution image of cholesterol molecules packed side-by-side with 0.5 nm spacing between neighbors and dimensions of a single cholesterol molecule determined from crystallographic data. The image was taken at $E = +0.2$ V, $E_{tip} = -0.15$ V, and $i_t = 6.0$ nA, within 10 min after the potential step from -0.6 to $+0.2$ V. The estimated concentration of cholesterol in the solution is 1.0×10^{-2} mM. The 0.05 M $KClO_4$ was used as the supporting electrolyte. (b) The same image after applying a low pass filter to remove contrast due to adsorbed molecules. The arrows indicate reconstruction lines of the gold surface.

of vesicles with metals finds application in the studies of cell adhesion and cell fusion.[29–31] It is also relevant for the understanding of biofilm formation, a significant issue in the food and in pulp and paper industries.[32,33]

Recently, we have applied STM to study the mechanism of 1,2-dimyristoyl-*sn*-glycero-3-phosphocholine (DMPC) vesicles spreading into a film at a Au(111) electrode surface.[28] We have demonstrated that fusion of vesicles is fast. However, instead of observing fragments of bilayers that move on the surface by sliding or rolling, we discovered that individual DMPC molecules spread over the surface and initially assemble into an ordered monolayer with acyl chains oriented parallel to the metal surface, similar to the monolayer formed by alkanes.[34] With time, the molecules reorient, and the monolayer is transformed into a thicker condensed film.

In the present paper, we will look at vesicles composed of 70 mol % DMPC and 30 mol % cholesterol. The objective of this study is to investigate the effect that cholesterol has on the mechanism of vesicle fusion at the Au(111) electrode surface. It is known that presence of cholesterol in the membrane of a vesicle results in a change of the membrane thickness and fluidity and causes a broadening of the gel-to-liquid crystalline phase transition.[35–37] We are interested in how the changes of these properties influence the mechanism of vesicles fusion at the gold surface. As a follow-up of our previous study of pure DMPC vesicles,[28] in this work, we employed the *in situ* electrochemical STM technique and recorded molecular resolution images as a function of time elapsed from the moment of

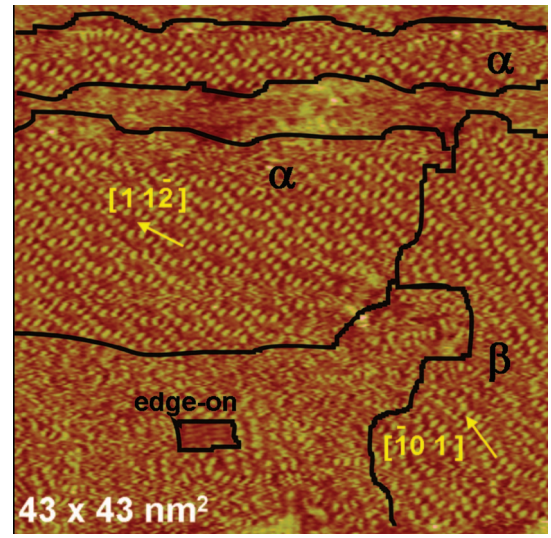

Figure 2. Image of an Au(111) electrode surface covered by a film of cholesterol formed in a solution of cholesterol suspension and recorded 60 min after the potential step from -0.6 to $+0.2$ V. The image was recorded at $E = +0.2$ V, $E_{tip} = -0.15$ V, and $i_t = 0.35$ nA. The image shows several ordered domains which boundaries are drawn with black lines. The estimated concentration of cholesterol in the solution is 1.0×10^{-2} mM. The 0.05 M $KClO_4$ was used as the supporting electrolyte.

(28) Xu, S.; Szymanski, G.; Lipkowski, J. *J. Am. Chem. Soc.* **2004**, *124*, 12276.
(29) Svetlicic, V.; Ivosevic, N.; Kovac, S.; Zutic, V. *Langmuir* **2000**, *16*, 8217.
(30) Svetlicic, V.; Ivosevic, N.; Kovac, S.; Zutic, V. *Bioelectrochemistry* **2000**, *53*, 79.
(31) Svetlicic, V.; Hozic, A *Electrophoresis* **2002**, *23*, 2080.
(32) (a) Screekumari, K. R.; Davey, L.; Leung, K. T.; Schraft, H.; Chen, A.; Low, N.; Truelstrup-Hansen, L.; Paulson, A.; Pink, D. *Microbiological and physicohemical characterization of paper mill biofilms, Biofilms2004: Structure and Activity of Biofilms* **2004**, 87−92. (b) Tian, M.; Kanavillil, N.; Davey, L.; Leung, K. T.; Schraft, H.; Chen, A. *J. Electroanal. Chem.* **2007**, *611*, 133.
(33) Busalmen, J. P.; Berna, A.; Feliu, J. M. *Langmuir* **2007**, *23*, 6459.
(34) (a) Yamada, R.; Uosaki, K. *J. Phys. Chem. B* **2000**, *104*, 6021. (b) Marchenko, O.; Cousty, J. *Phys. Rev. Lett.* **2000**, *84*, 5363. (c) Marchenko, O.; Cousty, J.; Van, L. P. *Langmuir* **2002**, *18*, 1171. (d) He, Y.; Ye, T.; Borguet, E. *J. Phys. Chem. B.* **2002**, *106*, 1264. (e) Xie, Z. X.; Xu, X.; Tang, J.; Mao, B. W. *J. Phys. Chem. B.* **2000**, *104*, 11719. (f) Xie, Z. X.; Huang, Z. F.; Xu, X. *Phys. Chem. Chem. Phys.* **2002**, *4*, 1486. (g) Zhang, H. M.; Xie, Z. X.; Mao, B. W.; Xu, X. *Chem. Eur. J.* **2004**, *10*, 1415.
(35) Dufourc, E. J.; Parish, E. J.; Chitrakorn, S.; Smith, I. C. P. *Biochemistry* **1984**, *23*, 6062.
(36) Vist, R. M.; Davis, H. J. *Biochemistry* **1990**, *29*, 451.
(37) Edidin, M. *Annu. Rev. Biophys. Biomol. Struct.* **2003**, *32*, 257.

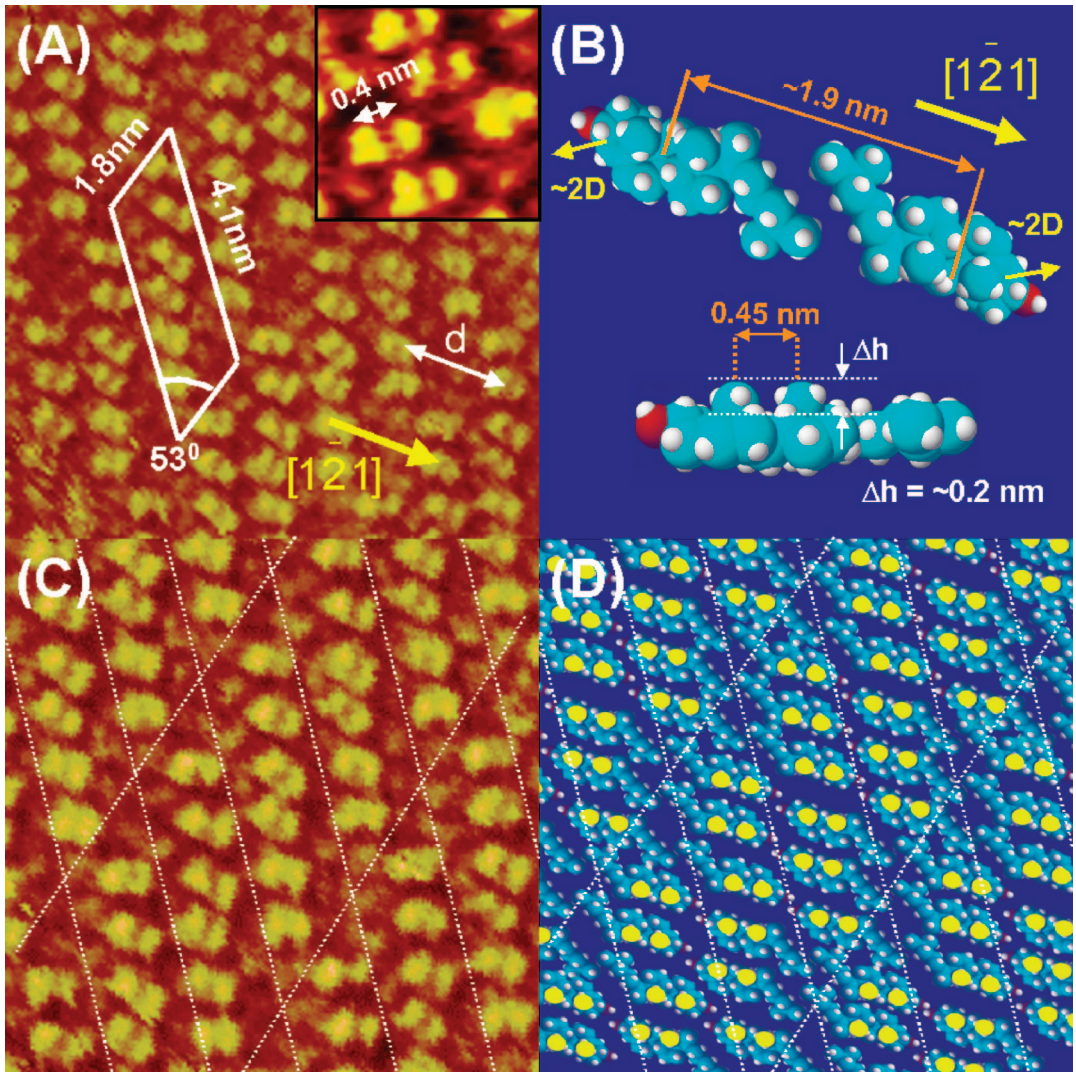

Figure 3. (A) High-resolution image of the α phase domain in the film of cholesterol at the Au(111) surface; inset is an enlarged fragment of the image showing the separation between the split spots that form the contrast in the STM image; (B) the orientation of cholesterol molecules with respect to the gold surface and a side view model of cholesterol showing the difference between the height of methyl groups and the sterol rings and a distance between the two methyl groups attached to the sterol rings; (C) higher resolution image of the α phase domain showing molecules packed into the 2D lattice; (D) molecular model giving the interpretation of the contrast in panel C. The STM images were taken at $E = +0.2$ V, $E_{tip} = -0.15$ V, and $i_t = 0.88$ nA. The estimated concentration of the cholesterol in the solution was 1.0×10^{-2} mM. The concentration of $KClO_4$ supporting electrolyte was 0.05 mM.

injection of a solution of DMPC/cholesterol vesicles into the electrochemical cell. To assist interpretation of our results, we also investigated the mechanism of spreading an aqueous suspension of pure cholesterol at the Au(111) surface. This work provides molecular level insights into the role of cholesterol in vesicles fusion at metals and first direct visualization of the dynamics of this process.

Experimental Section

The experiments were performed in 0.05 M $KClO_4$ (ACS Certified Fisher, Fair Lawn, NJ, twice recrystallized) solution. The Barenholtz procedure was used to prepare small unilamellar vesicles (SUVs) of a mixture of DMPC and cholesterol.[38] A 5.6 mg/mL chloroform solution of DMPC and a 1.5 mg/mL chloroform solution of cholesterol were used as the stock solutions. Appropriate volumes of the stock solutions were combined in a test tube to form a 7:3 (DMPC/cholesterol) mole fraction mixture. Then, the mixture was dried by vortexing under argon flow. To remove the residue of the solvent, dried mixture was placed in a vacuum desiccator for 2 h. Next, 3 mL of 0.05 M $KClO_4$ was added to the test tube, and the sample was sonicated at 35 °C for 1 h. The resulting transparent solution was injected into the electrochemical cell of the STM instrument in an amount which satisfied the desired final concentration. In the case of pure cholesterol, we followed exactly the same procedure, although in this case the final product was a fine suspension of cholesterol aggregates. Milli-Q ultrapure water (final resistivity ≥ 18.2 MΩ cm) was used to prepare all solutions. The glassware was cleaned in a hot mixture of HNO_3 and H_2SO_4 (1:3 v/v) for approximately 1 h and was then rinsed with large amounts of Milli-Q ultrapure water.

A small bead which was obtained by melting a gold wire according to Clavilier method[39] was used as the working electrode. The bead was spot-welded to a gold plate. The atomically flat (111) facets at the bead surface were used for image acquisition. A gold ring served as the counter electrode and a miniaturized Ag/AgCl (sat. KCl) was used as the reference electrode. The working electrode, the gold wire counter electrode, and the Teflon parts of the STM electrochemical cell were cleaned in piranha solution (concentrated H_2SO_4/30% H_2O_2 3:1 v/v) for 30 min and rinsed

(38) Barenholz, Y.; Gibbes, D.; Litman, B. J.; Goll, J.; Thompson, T. E.; Carlson, F. D. *Biochemistry* **1977**, *16*, 2806.
(39) Clavilier, J. *J. Electroanal. Chem.* **1980**, *107*, 211.

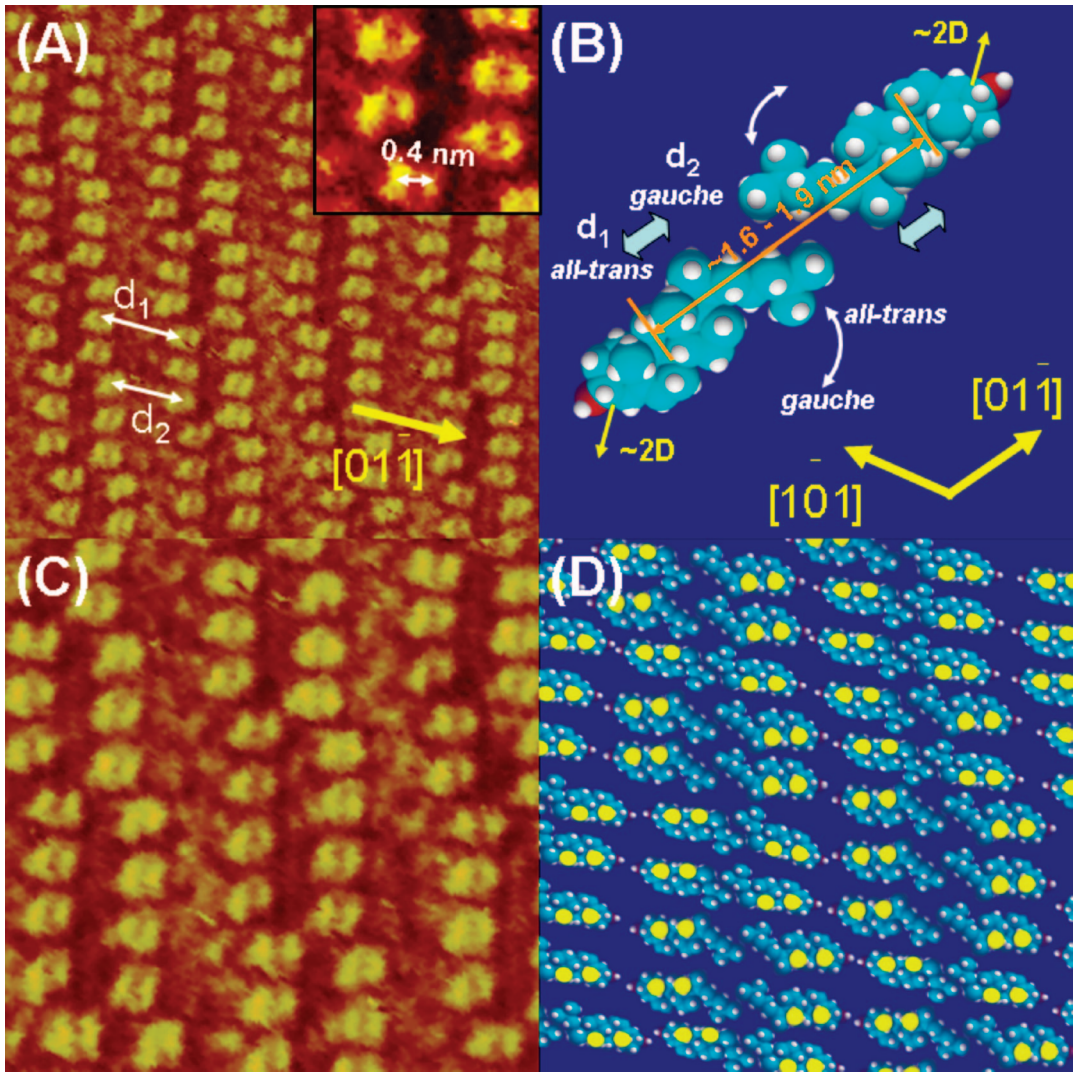

Figure 4. (A) High-resolution image of the β phase domain in the film of cholesterol at the Au(111) surface; inset is an enlarged fragment of the image showing the separation between the split spots that form the contrast in the STM image; (B) the orientation of cholesterol molecules with respect to the gold surface; (C) higher resolution image of the α phase domain showing molecules packed into the 2D lattice; (D) molecular model giving the interpretation of the contrast in panel C. The STM images were taken at $E = +0.2$ V, $E_{tip} = -0.15$ V, and $i_t = 1.3$ nA. The estimated concentration of cholesterol in the solution is 1.0×10^{-2} mM. The 0.05 M $KClO_4$ was used as the supporting electrolyte.

thoroughly with Milli-Q ultrapure water. (*CAUTION: piranha solution reacts violently with organic materials and should be handled with extreme care*). Gold electrodes (working and counter) were flame-annealed and quenched in Milli-Q water prior to assembly of the electrochemical cell.

The STM images were acquired using a Nanoscope II EC-STM connected to a Nanoscope IIIa controller (Digital Instruments, Santa Barbara, CA) with an A scanner. The constant current mode was used for imaging. The tungsten STM tips were electrochemically etched in a 2 M NaOH and then coated with polyethylene to minimize the faradaic currents. All images were recorded at the potential of +0.2 V versus Ag/AgCl, at which charge densities at the bare Au(111) surface and in the presence of the DMPC/cholesterol vesicles are about -5 $\mu C/cm^2$ and $+2$ $\mu C/cm^2$, respectively.[24] However, the solutions of pure cholesterol suspension and DMPC−cholesterol vesicles were added to the electrochemical cell at the potential of −0.6 V, where adsorption was not observed.[22–24,40] The potential was then stepped to +0.2 V, and the image acquisition was initiated. The differential capacitance curves illustrating the potential range where pure cholesterol and DMPC/cholesterol vesicles fuse and adsorb at the gold surface are shown in Figure 1 of the Supporting Information. The experiments were carried out at 19 ± 1°C.

The flame-annealed Au(111) electrode surface is reconstructed. A representative image of the reconstructed surface used in our experiments is shown in Figure 2 of the Supporting Information. The reconstructed Au(111) surface has characteristic parallel corrugation lines running along the [11$\bar{2}$] direction. The lines are arranged in pairs forming so-called reconstruction rows. The distances between twinned lines and between rows are 2.5 and 6.3 nm.[41,42] These dimensions were used for precise calibration of distances in the STM images. The line directions provided information concerning the crystallographic directions on the imaged surface.

Results and Discussion

Pure Cholesterol Film Formation. The studies described in this section were performed to assist the interpretation of images illustrating spreading of mixed DMPC−cholesterol vesicles.

(40) Bin, X.; Lipkowski, J. *J. Phys. Chem. B* **2006**, *110*, 26430.

(41) Gao, X.; Hamelin, A.; Weaver, M. *J. Phys. Chem.* **1991**, *95*, 6993.
(42) Kolb, D. M. *Prog. Surf. Sci.* **1996**, *51*, 109.

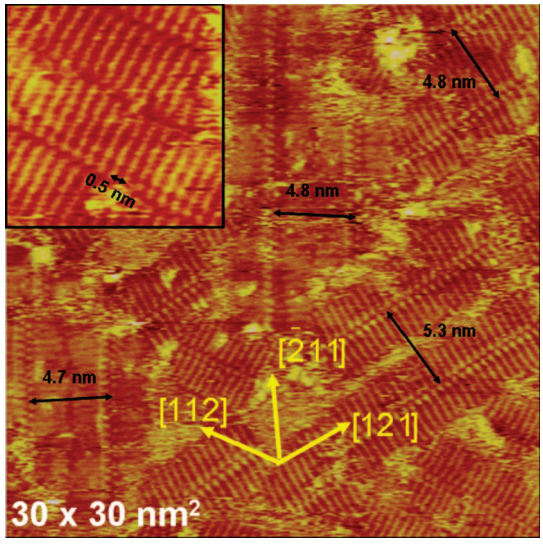

Figure 5. Image of a Au(111) electrode surface in a solution of mixed DMPC/cholesterol (7:3) vesicles acquired immediately after the potential step from −0.6 to +0.2 V. Inset is a high-resolution image showing acyl chains of DMPC molecules packed side-by-side with 0.5 nm spacing between neighbors. The imaging conditions: $E_{tip} = -0.15$ V, $i_t = 2.5$ nA. The estimated total concentration of DMPC/cholesterol in the solution is 3.1×10^{-2} mM. The 0.05 M $KClO_4$ was used as the supporting electrolyte.

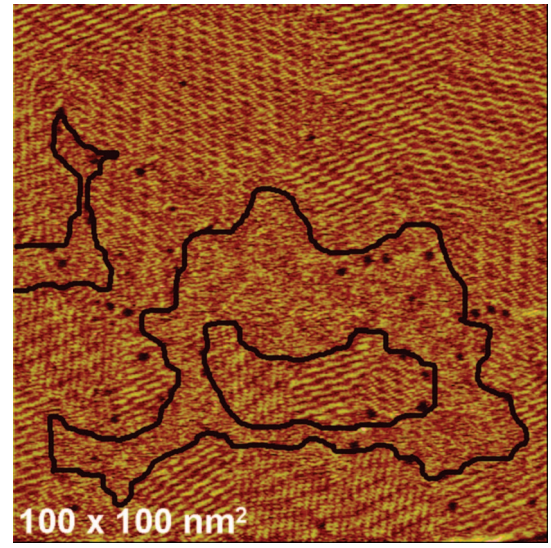

Figure 6. Image of a Au(111) electrode surface in a solution of mixed DMPC/cholesterol (7:3) vesicles acquired 6 min after the potential step from −0.6 to +0.2 V. Black lines mark boundaries between domains in the film of adsorbed molecules. The imaging conditions: $E_{tip} = -0.15$ V, $i_t = 0.36$ nA. The estimated total concentration of DMPC/cholesterol in the solution is 3.1×10^{-2} mM. The concentration of $KClO_4$ supporting electrolyte was 0.05 mM.

However, to facilitate further discussion, they are reported first. Figure 1A shows a representative image taken after injection of a cholesterol suspension into the STM cell. It reveals a characteristic stripe-like structure that usually appears 5−20 min after the potential step from −0.6 to +0.2 V versus Ag/AgCl. The width of these stripes is 3.8 ± 0.5 nm. The high-resolution image in the inset to Figure 1 indicates that the stripe-like structure consists of two rows of molecules oriented perpendicularly with respect to the stripe direction. The width of each row is 1.7 ± 0.3 nm, and the separation between neighboring molecules is about 0.5 ± 0.1 nm. Crystallographic data for anhydrous cholesterol show that eight cholesterol molecules are packed into a triclinic unit cell with dimensions $a = 1.4172$, $b = 3.4209$, and $c = 1.0481$nm, and the corresponding angles $\alpha = 95.5°$, $\beta = 90.0°$, and $\gamma = 96.32°$.[43] The second inset to Figure 1A, constructed with the help of the crystallographic data, shows that the length of an individual cholesterol molecule is ∼1.7nm, its width is ∼0.7nm, and its thickness is ∼0.5 nm. These numbers suggest that the contrast in Figure 1A is due to cholesterol molecules oriented with the longest *b* and the shortest *c* molecular axes parallel to the gold surface assuming the "edge-on" orientation.

Careful analysis of the STM image enables us to discern faint reconstruction lines of the underlying Au(111) surface. To expose the reconstruction lines, the STM image was filtered using Nanoscope 5.12r5 software and low pass filter. Figure 1B is the filtered image. The reconstruction lines marked with arrows are now clearly visible. With the help of this procedure the $[11\bar{2}]$, $[1\bar{2}1]$, and $[\bar{2}11]$ directions of the Au(111) surface could be determined. The adsorbed layer consists of several domains that are rotated by 60° or 120°. The molecular rows are oriented predominantly at an angle of ∼60° with respect to the direction of the reconstruction lines of the underlying gold surface. However, some molecular rows run in the direction parallel to the reconstruction line. Thus, cholesterol molecules are oriented predominantly along the nearest neighbor directions NN ($[1\bar{1}0]$,$[01\bar{1}]$,$[\bar{1}01]$) of the reconstructed Au(111) surface which ensures the most effective van der Waals interaction at the surface. Similar packing of molecules was observed for odd alkanes,[34,44] cationic surfactant DeTATf,[45] and DMPC[28] adsorbed on the Au(111) surface.

However, after 30–60 min, the structure of the film changed significantly. Figure 2 presents the image taken 60 min after the potential step to $E = +0.2$ V.

It shows the coexistence of four phases. Three of them marked α, β, and "edge-on" are ordered and one is disordered. The α phase was the most frequently observed structure in the STM images. In Figure 2, the small "edge-on" island is surrounded by the β phase. By counting the number of spots per unit area, one can determine that the β phase has about 10–15% higher packing density. The image in Figure 2 was also filtered to determine directions of the reconstruction lines and crystallographic directions of the underlying gold surface. This procedure revealed that the bright spots in Figure 2 are preferentially oriented along $[1\bar{2}1]$ and $[11\bar{2}]$ directions in the case of α phase and along $[01\bar{1}]$ and $[\bar{1}01]$ directions in the case of β phase. This behavior indicates that the Au(111) surface acts as a template for packing of cholesterol molecules in α and β phases as well.

Figure 3A is a zoomed image of the α phase domain. It shows a well-defined two-dimensional (2D) lattice whose unit cell is defined by two vectors which are 1.8 ± 0.2 and 4.1 ± 0.3 nm long, with a 53 ± 3° angle between these vectors. The longer vector is preferentially oriented along $[11\bar{2}]$ direction, and in some cases it is aligned with $[\bar{2}11]$ direction of the underlying Au(111) surface. The area of the unit cell is equal to 6.0 ± 0.6 nm^2. The contrast shows six pairs of bright spots within one

(43) Shieh, H. S.; Hoard, L. G.; Nordman, C. E. *Nature* **1977**, *267*, 287.
(44) Uosaki, K.; Yamada, R. *J. Am. Chem. Soc.* **1999**, *121*, 4090.
(45) Sek, S.; Chen, M.; Brosseau, C. L.; Lipkowski, J. *Langmuir* **2007**, *23*, 12529.

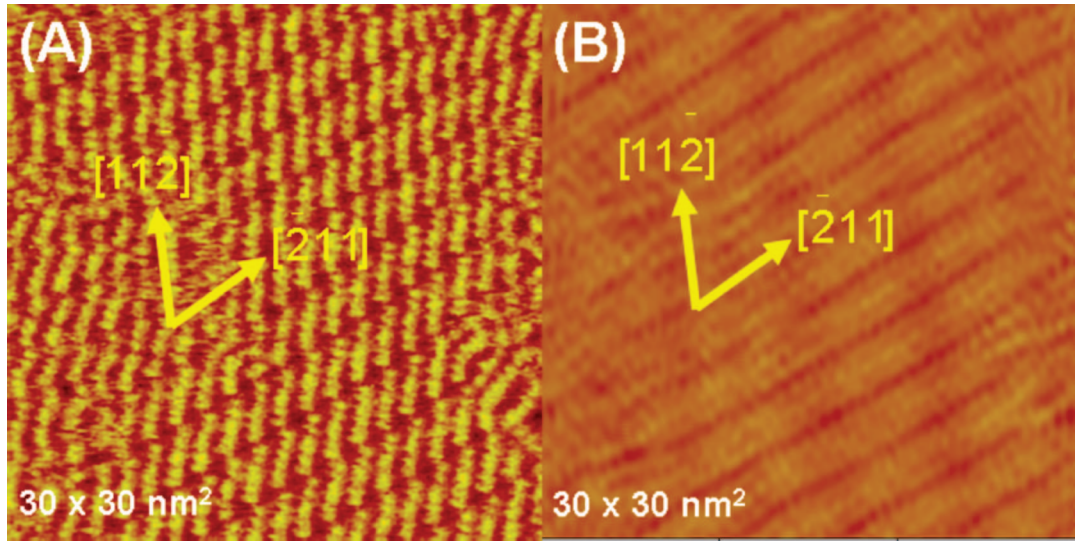

Figure 7. High-resolution image of one ordered domain of the film formed at the Au(111) electrode surface in contact with the solution of mixed DMPC/cholesterol (7:3) vesicles recorded 6 min after stepping the potential from −0.6 to +0.2 V. (B) the same image after digital filtering of bright spots that form the contrast in panel A. The imaging conditions: $E_{tip} = -0.15$ V, $i_t = 0.36$ nA. The estimated total concentration of DMPC/cholesterol in the solution is 3.1×10^{-2} mM. The 0.05 M $KClO_4$ was used as the supporting electrolyte.

unit cell. The area per one pair of spots is therefore equal to 1.0 ± 0.1 nm^2. Incidentally, according to the crystallographic data, the product of the length and the width of one cholesterol molecule can vary from 1.0 to 1.2 nm^2, see ref 43, 46.

Furthermore, the distance between the two bright spots in a pair is 0.4 ± 0.1 nm. The side view model in Figure 3B shows that this distance is in a good agreement with the distance between the two methyl groups of a cholesterol molecule which is 0.45 nm. The model also shows that the two methyl groups protrude by 0.2 nm from the sterol rings and are the two highest points on flat lying molecule. These numbers suggest that the pairs of bright spots that form the contrast in Figure 3A represent methyl groups of flat lying cholesterol molecules.

Figure 3B shows that the flat lying molecules are arranged into pairs of cholesterol molecules oriented tail to tail. The direction of the long axes of the two molecules is parallel to the $[1\bar{2}1]$ direction which corresponds to the next nearest neighbor NNN direction of atoms on the underlying gold surface. In the flat configuration, the distance between methyl groups of the two opposing molecules in the pair amounts to ~1.9 nm. This number is equal to the distance d between the bright spots marked in Figure 3A (the distribution of the distances for α phase is shown in Figure 3 in Supporting Information). Figure 3C shows an enlarged image of the α phase which is used to demonstrate how cholesterol molecules are packed in this structure. The dotted lines mark the 2D lattice of this adlayer. The model in Figure 3D shows the packing of the cholesterol molecules into the 2D lattice. The lattice is formed by six cholesterol molecules occupying one unit cell. The first three molecules are oriented in parallel, but the remaining three assume an inverted (mirror image) orientation. This inversion explains the bend in the row of six split bright spots in the unit cell of images in panels A and C of Figure 3. In this structure, all molecules assume a head-to-head and tail-to-tail orientation and their permanent dipole moments are directed chiefly antiparallel. The model presented in Figure 3D can be superimposed on the image in Figure 3C by a horizontal translation reproducing the contrast very well.

(46) Craven, B. M. *Nature* **1976**, *260*, 727.

Figure 4A is a zoomed image of the β phase domain. In this phase, cholesterols are ordered into rows of head-to-head and tail-to-tail oriented molecules, but the adlayer lacks periodicity, and hence, the unit cell of this structure cannot be determined. The lack of periodicity results from irregular changes of the width of these rows. The image shows that the distance between the bright spots that determine the width of the row is equal to either $d_1 = 1.9 \pm 0.1$ nm or $d_2 = 1.6 \pm 0.1$ nm, and these numbers vary irregularly along the rows (for the distribution of the distances see Figure 4 in Supporting Information). Figure 4B−D gives the interpretation of the contrast in the STM image. Figure 4B shows that packing of molecules within this structure is somewhat different than that of the α phase. The long axes of the flat-lying cholesterol molecules are aligned with the $[1\bar{1}0]$ which is the nearest neighbor NN direction at the reconstructed Au(111) electrode surface. The shortening of the distance between the bright spots corresponding to opposing cholesterol molecules may be explained by a rotation of the tail to a gauche conformation. This allows a ~10% higher packing density in the adlayer. Figure 4C is an enlarged image of the β phase, and Figure 4D is showing the packing of the cholesterol molecules in this structure. The model can be superposed onto the image in Figure 4C by a horizontal translation reproducing the contrast very well.

In general, the multiplicity of 2D structures observed in the STM images reflects the fact that the self-assembly of cholesterol molecules at the Au(111) surface involves competition between molecule−molecule and molecule−substrate interactions. These are weak van der Waals interactions; the energetic differences between various structures are small, and therefore, various structures coexist at the surface.

Spreading of Mixed DMPC/Cholesterol Vesicles. In this section, we present the main result of this study that concerns the mechanism of spreading of unilamellar DMPC/cholesterol (7:3) vesicles. Figure 5 shows the STM image recorded after injection of the DMPC/cholesterol (7:3) vesicles into the electrochemical cell of the EC-STM apparatus. The image was taken a few minutes after stepping the potential from −0.6 to +0.2 V. The characteristic stripe-like adlayer, similar to that shown in Figure 1, appeared 1−5 min after stepping the

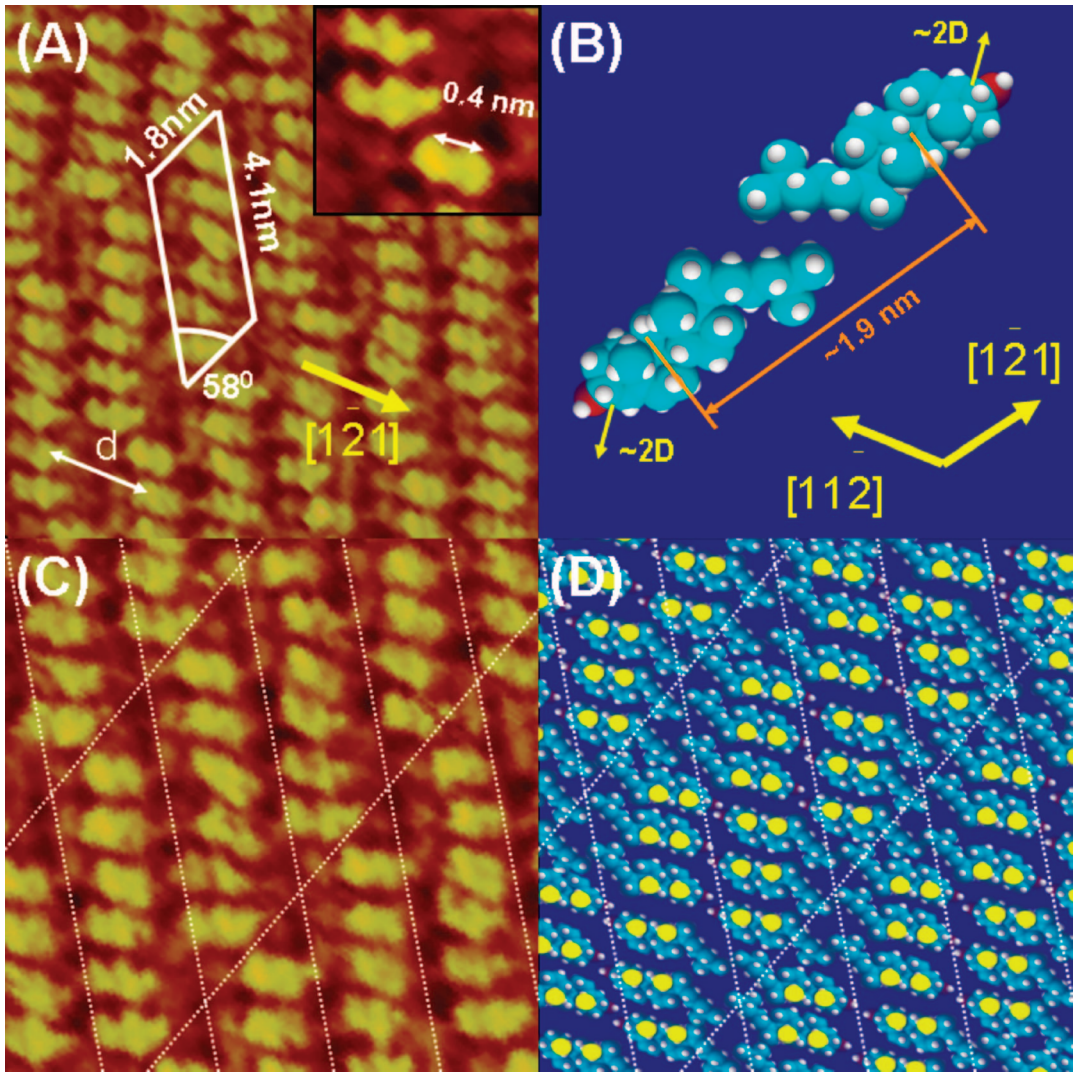

Figure 8. (A) High-resolution image of the ordered domain formed at the Au(111) electrode surface in contact with the solution of mixed DMPC/cholesterol (7:3) vesicles recorded 6 min after stepping the potential from −0.6 to +0.2 V; inset is an enlarged fragment of the image showing the separation between the split spots that form the contrast in the STM image; (B) the orientation of cholesterol molecules with respect to the gold surface; (C) higher resolution image of the domain showing molecules packed into the 2D lattice; (D) molecular model giving the interpretation of the contrast in panel C. Imaging conditions: $E_{tip} = -0.15$ V, $i_t = 0.45$ nA. The estimated total concentration of the DMPC/cholesterol in the solution is 3.1×10^{-2} mM. The 0.05 M $KClO_4$ was used as the supporting electrolyte.

potential. The high-resolution image in the inset to Figure 5 shows that each stripe consists of two rows of flat-lying molecules, oriented perpendicularly with respect to the stripe direction. The separation between the neighboring molecules is 0.5 ± 0.1 nm. The stripes are aligned with [11$\bar{2}$], [1$\bar{2}$1], [$\bar{2}$11] directions, which means that the molecular axis are oriented along [1$\bar{1}$0], [$\bar{1}$01], [01$\bar{1}$] NN directions, respectively.

The stripes have an average width of 4.7 ± 0.4 nm which is significantly larger than the width of the stripes observed in Figure 1, for cholesterol molecules. However, this number is in a good agreement with the width of similar stripes formed during the fusion of pure DMPC vesicles which was equal to 4.4 ± 0.2 nm.[28] No features that could be identified as shorter cholesterol molecules positioned between longer DMPC molecules were observed in Figure 5. Therefore, Figure 5 shows an image of a DMPC-rich adlayer that is formed at the initial stage of spreading of mixed DMPC/cholesterol vesicles. It is essentially identical with the adlayer previously observed for spreading pure DMPC vesicles.[28]

The stripe-like structure seen in Figure 5 was stable for 3–15 min. With time, the adlayer was transformed, and a new structure appeared which is shown in Figure 6. In this image, several large ordered and disordered domains coexist. The ratio of the area occupied by the ordered and the disordered phases varied widely when images were acquired from different spots on the surface. Since the STM images of the film formed by fusion of pure DMPC vesicles reported earlier[28] did not display similar structures, we can conclude that the formation of the new ordered domains seen in Figure 6 is due to the presence of cholesterol.

Careful analysis of the image in Figure 6 shows that the ordered region consists of several domains which represent the same structure rotated by 120°. The image also shows faint but discernible chevron-like lines characteristic of a reconstructed Au(111) surface. The presence of the reconstruction lines could be better seen in Figure 7. Figure 7A shows one ordered domain, while Figure 7B shows the same image after the arrays of spots were filtered by the digital image processing. The reconstruction

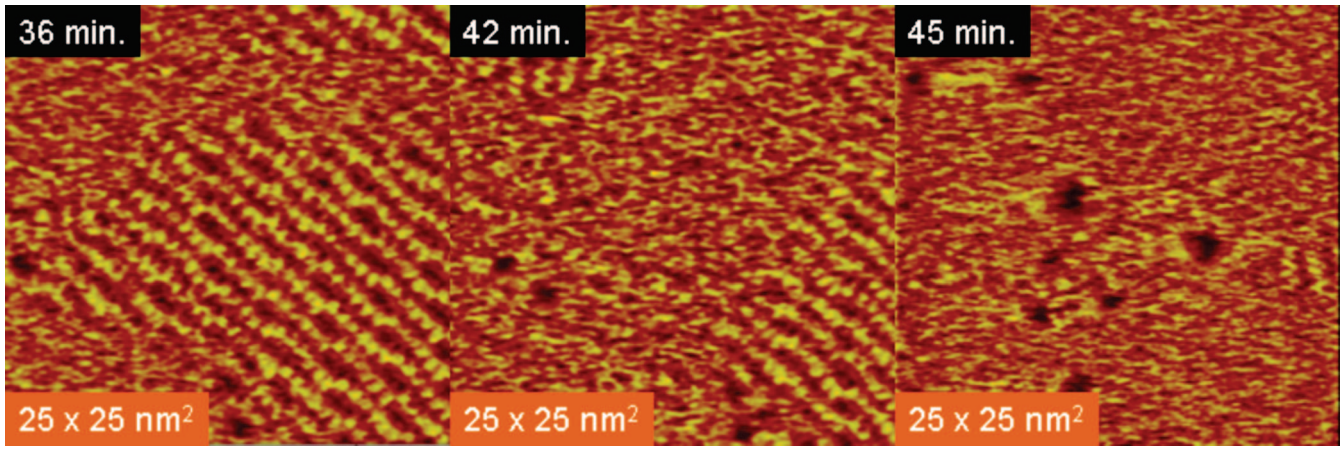

Figure 9. Evolution of the film structure with time. Images of a Au(111) electrode surface in a solution of mixed DMPC/cholesterol (7:3) vesicles acquired 36, 42, and 45 min after the potential step from −0.6 to +0.2 V, respectively. Imaging conditions: $E_{tip} = -0.15$ V, $i_t = 0.25$ nA. The estimated total concentration of DMPC/cholesterol in the solution is 3.1×10^{-2} mM. The 0.05 M $KClO_4$ was used as the supporting electrolyte.

lines are clearly visible in this image, and by using them as a reference, one can determine that the rows of bright spots that form the contrast in Figure 7A are aligned in the $[\bar{2}11]$ direction. Thus, the structure seen in Figures 6 and 7 is templated by the underlying gold surface.

The detailed analysis of this structure is shown in Figure 8. The high-resolution images in Figure 8A,C show that the adlayer forms characteristic 2D lattice with the unit cell defined by two vectors which are 1.8 ± 0.3 and 4.1 ± 0.6 nm long, and $58 \pm 4°$ angle between these vectors. This is the same lattice that was observed earlier in Figure 3 for pure cholesterol molecules. Further, the lattice contains six pairs of split bright spots separated by 0.4 ± 0.1 nm, and the longer separation between the spots d is equal to 1.9 ± 0.2 nm which is in good agreement with the distances between the spots observed in Figure 3 (for the distribution of the distances see Figure 5 in Supporting Information). Therefore, we can safely conclude that the ordered structures seen in Figures 6−8 are due to patches of pure cholesterol molecules that are adsorbed flat at the surface and form a structure previously described as the α phase. Figure 8B shows the tail-to-tail arrangements of two flat-laying cholesterol molecules along the distance d. The molecules are oriented parallel to the $[1\bar{2}1]$ direction which is the NNN direction of the underlying gold surface. Figure 8D shows how cholesterol molecules are packed in the 2D lattice. This is the same packing that was previously described for α phase of the pure cholesterol adlayer. The model in Figure 8D can be superposed on the image in Figure 8C reproducing the contrast very well.

However, the structure observed in Figure 8 was temporary and was only stable within a ∼30 min time window. Figure 9 shows that this structure disappears with time and is transformed into a featureless film. However, when the potential is stepped to −0.6 V to detach the film and then back to +0.2 V, the structure seen in Figures 6−8 reappears again.

This behavior indicates that a segregation of cholesterol and DMPC into one component domains takes place at early stages of the mixed film formation. To determine the nature of the featureless film formed after ∼60 min, additional atomic force microscopy experiments were performed. The force–distance curves were recorded, and the thickness of the film was determined to be 4.5 ± 0.5 nm (see Supporting Information). This number indicates that the featureless film formed after long incubation time is a bilayer. Independently, neutron reflectivity studies[22] demonstrated that indeed a bilayer is formed at the gold electrode surface by fusion of the mixed DMPC/cholesterol vesicles.

Conclusions

The experiments described in this work confirm results of our earlier studies,[28] in that there are remarkable differences between the mechanism of phospholipid bilayer formation, by spreading of unilamellar vesicles, at hydrophobic metals such as gold and at hydrophilic surfaces of quartz, glass, or mica. No evidence was observed that vesicle fusion occurs by releasing fragments of the bilayer which later spread by sliding or rolling at the gold surface. Clearly, such motion requires a thin lubricating film of the solvent present at a hydrophilic surface. In contrast, at the hydrophobic metal surface, the molecules released by rupture of a vesicle initially self-assemble into a well-ordered monolayer. The self-assembly is controlled by the hydrocarbon skeleton−metal surface interaction. A fascinating result of the present study with mixed DMPC/cholesterol vesicles is the observation that the molecule−metal interactions induce segregation of the two-component mixture into single components of either cholesterol or DMPC-rich domains. However, the molecule−metal interaction induced monolayer is a transient phenomenon. When more molecules accumulate at the surface, the molecule−molecule interactions start to dominate the assembly, and the monolayer is then transformed into a bilayer.

Acknowledgment. This work has been supported by a grant from the Natural Sciences and Engineering Council of Canada. J.L. acknowledges the Canada Foundation for Innovation for the Canada Research Chair Award.

Supporting Information Available: The differential capacitance curves for a Au(111) electrode in the presence of cholesterol and DMPC/cholesterol vesicles, details of calibration of the distances using reconstruction lines on a Au(111) surface, and determination of the crystallographic directions and preliminary AFM data. This material is available free of charge via the Internet at http://pubs.acs.org.

JA711020Q